Encapsulated subwavelength grating as a quasi-monolithic resonant reflector

Frank Brückner,[1,*] Daniel Friedrich,[2] Michael Britzger,[2] Tina Clausnitzer,[1] Oliver Burmeister,[2] Ernst-Bernhard Kley,[1] Karsten Danzmann,[2] Andreas Tünnermann,[1] and Roman Schnabel[2]

[1] *Institut für Angewandte Physik, Friedrich-Schiller-Universität Jena, Max-Wien-Platz 1, 07743 Jena, Germany*
[2] *Max-Planck-Institut für Gravitationsphysik (Albert-Einstein-Institut) and Institut für Gravitationsphysik, Leibniz Universität Hannover, Callinstrasse 38, 30167 Hannover, Germany*

roman.schnabel@aei.mpg.de

Abstract: For a variety of laser interferometric experiments, the thermal noise of high-reflectivity multilayer dielectric coatings limits the measurement sensitivity. Recently, monolithic high-reflection waveguide mirrors with nanostructured surfaces have been proposed to reduce the thermal noise in interferometric measurements. Drawbacks of this approach are a highly complicated fabrication process and the high susceptibility of the nanostructured surfaces to damage and pollution. Here, we propose and demonstrate a novel quasi-monolithic resonant surface reflector that also avoids the thick dielectric stack of conventional mirrors but has a flat and robust surface. Our reflector is an encapsulated subwavelength grating that is based on silicon. We measured a high reflectivity of 93 % for a wavelength of $\lambda = 1.55\,\mu$m under normal incidence. Perfect reflectivities are possible in theory.

© 2009 Optical Society of America

OCIS codes: (050.2770) Gratings; (050.6624) Subwavelength structures; (230.3990) Micro-optical devices; (230.4040) Mirrors.

References and links

1. P. F. Cohadon, A. Heidmann, and M. Pinard, "Cooling of a Mirror by Radiation Pressure," Phys. Rev. Lett. **83,** 3174–3177 (1999).
2. T. Corbitt, Y. Chen, E. Innerhofer, H. Müller-Ebhardt, D. Ottaway, H. Rehbein, D. Sigg, S. Whitcomb, C. Wipf, and N. Mavalvala, "An All-Optical Trap for a Gram-Scale Mirror," Phys. Rev. Lett. **98,** 150802 (2007).
3. H. Müller-Ebhardt, H. Rehbein, R. Schnabel, K. Danzmann, and Y. Chen, "Entanglement of Macroscopic Test Masses and the Standard Quantum Limit in Laser Interferometry," Phys. Rev. Lett. **100,** 013601 (2008).
4. H. J. Kimble, Y. Levin, A. B. Matsko, K. S. Thorne, and S. P. Vyatchanin, "Conversion of conventional gravitational-wave interferometers into quantum nondemolition interferometers by modifying their input and output optics," Phys. Rev D. **65,** 022002 (2001).
5. P. Aufmuth and K. Danzmann, "Gravitational wave detectors," New J. Phys. **7,** 202 (2005).
6. G. M. Harry, A. M. Gretarsson, P. R. Saulson, S. E. Kittelberger, S. D. Penn, W. J. Startin, S. Rowan, M. M. Fejer, D. R. M. Crooks, G. Cagnoli, J. Hough, and N. Nakagawa, "Thermal noise in interferometric gravitational wave detectors due to dielectric optical coatings," Class. Quantum Grav. **19,** 897–917 (2002).
7. D. R. M. Crooks, P. Sneddon, G. Cagnoli, J. Hough, S. Rowan, M. M. Fejer, E. Gustafson, R. Route, N. Nakagawa, D. Coyne, G. M. Harry and A. M. Gretarsson, "Excess mechanical loss associated with dielectric mirror coatings on test masses in interferometric gravitational wave detectors," Class. Quantum Grav. **19,** 883-896 (2002).
8. K. Numata, A. Kemery, and J. Camp, "Thermal-Noise Limit in the Frequency Stabilization of Lasers with Rigid Cavities," Phys. Rev. Lett. **93,** 250602 (2004).

#120315 - $15.00 USD Received 23 Nov 2009; revised 16 Dec 2009; accepted 17 Dec 2009; published 18 Dec 2009

9. Y. Levin, “Internal thermal noise in the LIGO test masses: A direct approach,” Phys. Rev. D **57,** 659–663 (1998).
10. G. Rempe, R. J. Thompson, H. J. Kimble, R. Lalezari, “Measurement of ultralow losses in an optical interferometer,” Opt. Lett. **17**, 363–365 (1992).
11. G. A. Golubenko, A. S. Svakhin, V. A. Sychugov, and A. V. Tishchenko, “Total reflection of light from a corrugated surface of a dielectric waveguide,” Sov. J. Quantum Electron. **15,** 886–887 (1985).
12. R. Magnusson and S. S. Wang, “New principle for optical filters,” Appl. Phys. Lett. **61,** 1022–1024 (1992).
13. A. Sharon, D. Rosenblatt, and A. A. Friesem, “Resonant grating-waveguide structures for visible and near-infrared radiation,” J. Opt. Soc. Am. A **14,** 2985–2993 (1997).
14. R. Nawrodt, A. Zimmer, T. Koettig, T. Clausnitzer, A. Bunkowski, E.-B. Kley, R. Schnabel, K. Danzmann, W. Vodel, A. Tünnermann, and P. Seidel, “Mechanical Q-factor measurements on a test mass with a structured surface,” New J. Phys. **9,** 225 (2007).
15. T. Clausnitzer, A. V. Tishchenko, E.-B. Kley, H.-J. Fuchs, D. Schelle, O. Parriaux, and U. Kroll, “Narrowband, polarization-independent free-space wave notch filter,” J. Opt. Soc. Am. A **22,** 2799–2803 (2005).
16. A. Bunkowski, O. Burmeister, D. Friedrich, K. Danzmann, and R. Schnabel, “High reflectivity grating waveguide coatings for 1064 nm,” Class. Quantum Grav. **23,** 7297–7303 (2006).
17. C. F. R. Mateus, M. C. Y. Huang, L. Chen, C. J. Chang-Hasnain, and Y. Suzuki, “Broad-Band Mirror (1.12 - 1.62 μm) Using a Subwavelength Grating,” IEEE Phot. Techn. Lett. **16,** 1676–1678 (2004).
18. F. Brückner, D. Friedrich, T. Clausnitzer, O. Burmeister, M. Britzger, E.-B. Kley, K. Danzmann, A. Tünnermann, and R. Schnabel, “Demonstration of a cavity coupler based on a resonant waveguide grating,” Opt. Express **17,** 163–169 (2009).
19. G. Cella and A. Giazotto, ”Coatingless, tunable finesse interferometer for gravitational wave detection,” Phys. Rev D. **74**, 042001 (2006).
20. S. Goßler, J. Cumpston, K. McKenzie, C. M. Mow-Lowry, M. B. Gray, and D. E. McClelland, ”Coating-free mirrors for high precision interferometric experiments,” Phys. Rev A. **76**, 053810 (2007).
21. F. Brückner, T. Clausnitzer, O. Burmeister, D. Friedrich, E.-B. Kley, K. Danzmann, A. Tünnermann, and R. Schnabel, ”Monolithic dielectric surfaces as new low-loss light-matter interfaces,” Opt. Lett. **33**, 264-266 (2008).
22. P. Lalanne and D. Lemercier-Lalanne, ”On the effective medium theory of subwavelength periodic structures,” J. Mod. Opt. **43**, 2063 (1996).
23. T. Clausnitzer, T. Kämpfe, E.-B. Kley, A. Tünnermann, U. Peschel, A. V. Tishchenko, and O. Parriaux, “An intelligible explanation of highly-efficient diffraction in deep dielectric rectangular transmission gratings,” Opt. Express **13,** 10448–10456 (2005).
24. M. G. Moharam and T. K. Gaylord, “Rigorous coupled-wave analysis of planar-grating diffraction,” J. Opt. Soc. Am. **71,** 811–818 (1981).
25. T. Clausnitzer, T. Kämpfe, F. Brückner, R. Heinze, E.-B. Kley, and A. Tünnermann, ”Reflection-reduced encapsulated transmission grating,” Opt. Lett. **33,** 1972–1974 (2008).
26. J. Nishii, K. Kintaka, and T. Nakazawa, ”High-efficiency transmission gratings buried in a fused-SiO_2 glass plate,” Appl. Opt. **43,** 1327–1330 (2004).

1. Introduction

During the past decades high-precision interferometric experiments were pushed towards an ultimate sensitivity regime where quantum effects are starting to play a decisive role. In these ongoing and future experiments, such as laser cooling of mechanical oscillators [1], optical traps for mirrors [2], generation of entangled test masses [3], quantum non-demolition interferometry [4], gravitational wave detection [5, 6, 7], and frequency stabilization of lasers with rigid cavities [8], light and matter act as an opto-mechanical system. The surface of the (high quality) mechanical oscillator has to be a light/matter interface with outstanding high reflectivity and high mechanical quality factor to reduce the influence of thermal noise [9]. Monocrystalline materials such as quartz or silicon are used to reach high mechanical quality factors; multilayer dielectric coatings are commonly used to provide high optical quality. The most commonly used materials for these coatings are SiO_2 and Ta_2O_5. Reflectivities of dielectric multilayer coatings of up to 99.9998 % have been demonstrated [10]. However, recent theoretical and experimental research revealed that multilayer coatings result in a significant reduction of *mechanical* quality factors. This effect is mainly caused by internal friction of the alternately coated layers [6, 7, 9]. Thus, the so-called ’coating thermal noise’ has become a major noise source in opto-mechanical systems.

A promising approach being pursued to design alternative mirror architectures with reduced

#120315 - $15.00 USD Received 23 Nov 2009; revised 16 Dec 2009; accepted 17 Dec 2009; published 18 Dec 2009
(C) 2009 OSA

thermal noise is based on surface relief guided-mode resonant waveguide gratings [11, 12, 13]. They comprise only a single but periodically corrugated high refractive index layer on top of a low refractive index substrate. Recently it was experimentally shown that a periodic corrugation etched into the surface of a substrate did not reduce the substrate's quality factor, which was of the order 10^8 [14]. Although these resonant grating structures were initially intended to act as narrowband filtering or switching devices [12, 15], they can also be advanced to broadband reflectors by means of particular parameter design [16, 17, 18]. However, for the fabrication of such devices still one layer of a material other than the substrate is involved which potentially decreases the high mechanical quality of the substrate material. Thus, a coating-free (i.e. monolithic) mirror concept is of enormous interest. Previous published approaches [19, 20] are based on total internal reflection which is connected with additional optical paths inside a substrate giving rise to absorption and increased thermo-refractive noise resulting from a temperature dependent index of refraction. Very recently, we proposed to advance the waveguide grating configuration to a monolithic surface mirror that solely consists of a single silicon crystal [21]. However, the highly complicated grating profile implies a challenging fabrication process as well as severe restrictions in the device handling.

Here, we propose and demonstrate a quasi-monolithic mirror architecture that is formed by an encapsulated subwavelength grating. Such a device also creates a resonant waveguide structure, but with a flat and robust surface. This configuration offers new benefits for the handling and the fabrication process. Once fabricated the device is protected against mechanical damage and also against contamination, since its surface can be cleaned in the same manner as a conventional polished surface. This approach for a monolithic mirror has, to the best of our knowledge, never been suggested before. We present a design that is based on rigorous simulations and a first demonstrator fabricated from silicon. Our measurement results revealed a promising high reflectivity of 93 % for normal incidence at the design wavelength of $\lambda = 1550$ nm.

2. Guided-mode resonant waveguide gratings

For resonant waveguide grating structures, high reflectivity is being facilitated by resonant light coupling instead of multiple interference in case of dielectric multilayer coatings. Here, a low refractive index substrate carries a single waveguide (high refractive index) layer that is periodically nanostructured. The fundamental principle of waveguide grating structures is illustrated in Fig. 1(a) and can be described by a simple ray picture [13]. In order to allow for resonant reflection under normal incidence, the corrugation period need to fulfill the following parameter inequality (which can be derived from the well-known grating equation):

$$\lambda/n_{\mathrm{H}} < d < \lambda/n_{\mathrm{L}}\,, \qquad (1)$$

where d is the grating period, λ is the light's vacuum wavelength, and n_{H} and n_{L} are the higher and lower refractive indices, respectively. In this simplified ray picture, the first diffraction orders (-1T, +1T) in the high-index layer experience total internal reflection (at the interface to the low-index substrate) and, thus, excite resonant waveguide modes propagating along the corrugated high-index layer. A part of the light inside the waveguide is coupled out via the grating to both, the transmitted and reflected zeroth order (0R, 0T). If the grating period d, the groove depth g, the grating fill factor f (ratio between ridge width r and grating period d), and the high-index layer thickness s with respect to the refractive index values of the involved materials are designed properly, all transmitted light can be prompted to interfere destructively, corresponding to a theoretical 100 % reflectance. Depending on whether the coupling efficiency to the waveguide modes within the high-index layer is low or high, the reflector shows a narrow or a broad spectral reflectance, respectively [13]. By means of particular grating parameter design

#120315 - $15.00 USD Received 23 Nov 2009; revised 16 Dec 2009; accepted 17 Dec 2009; published 18 Dec 2009
(C) 2009 OSA

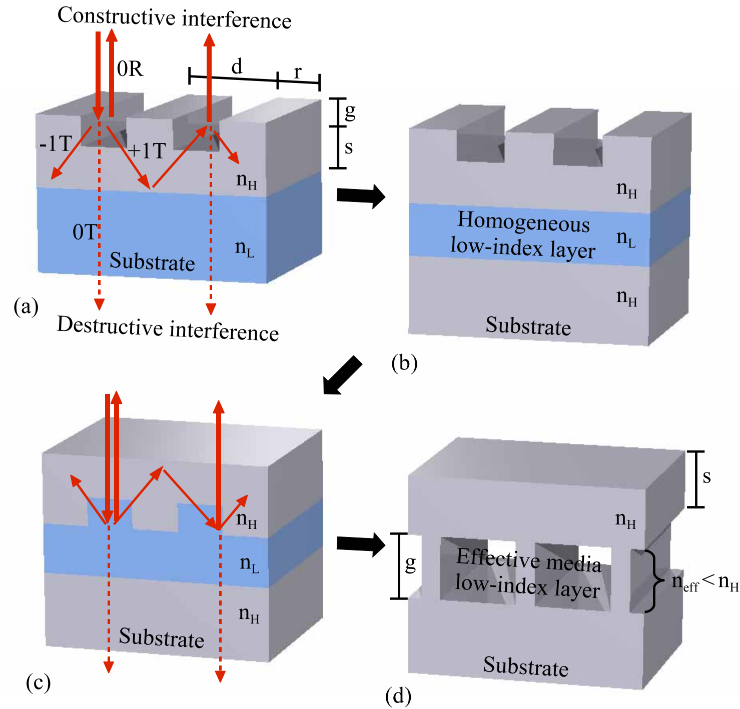

Fig. 1. (a) Initial waveguide grating configuration and its fundamental principle in a simplified ray picture (see main text for explanation), (b) reduction of the low-index substrate to a low-index layer, (c) movement of the grating region beneath the waveguide layer to supply a flat surface, (d) replacement of the homogeneous by an effective media low-index layer to provide a purely monolithic mirror architecture. The light rays in (c) illustrate how the waveguide modes are excited in reflection when the grating is beneath the waveguide layer (light rays have been omitted in (b) and (d) for clarity).

and providing a high refractive index contrast between both involved materials, the coupling efficiency can be increased, whereby the spectral response is significantly broadened.

Figure 1(b) shows a configuration of a resonant reflector for a high refractive index material such as silicon ($n = 3.48$ at the wavelength of 1550 nm). In this situation, a low refractive index layer beneath the waveguide grating is indispensable [17]. This cladding layer needs to have a certain minimum thickness in order to prevent evanescent transmission of higher diffraction orders to the substrate. The waveguide grating in Fig. 1(b) can be changed to a flat surface configuration by simply moving the top grating region beneath the waveguide layer as shown in Fig. 1(c). Here, the resonant waveguide modes are excited by reflected higher diffraction orders as indicated by the light rays.

3. Monolithic implementation

Similar to the approach in Ref. [21], Fig. 1 can be understood as a stepwise transition from the initial surface corrugated resonant waveguide mirror (a) to, finally, our flat surface encapsulated grating waveguide mirror. In Fig. 1(d) we propose to replace the homogeneous low-index layer in (c) by an *effective* low-index layer (which has an effective index $n_{\mathrm{eff}} < n_{\mathrm{H}}$) thereby enabling a truly monolithic configuration of a resonant reflector with a flat, uncorrugated surface. This effective low-index grating layer needs to exhibit the same period as the grating in Fig. 1(c) in

#120315 - $15.00 USD Received 23 Nov 2009; revised 16 Dec 2009; accepted 17 Dec 2009; published 18 Dec 2009
(C) 2009 OSA

order to fulfill Ineq. (1) that allow for resonant reflection in principle. Since it is supposed to generate higher diffraction orders (in reflection), the realization of the introduced grating as an effective medium is not obvious [22]. Only if the grating fill factor is sufficiently low, no higher diffraction orders are allowed to propagate to the substrate material as required, according to Ineq. (1).

We note that the electromagnetic field inside this encapsulated periodic structure can be expressed by discrete grating modes [23]. These modes correspond to the diffraction orders within a conventional resonant waveguide grating. Similar to the higher diffraction orders within a conventional waveguide layer, the resonant excitation of these modes can result in a destructive interference of all light transmitted to the effective layer. Thus, the monolithic encapsulated grating, as depicted in Fig. 1(d), can be optimized to create 100 % reflectivity.

4. Encapsulated grating design considerations

The design parameters of our encapsulated grating reflector were optimized for a broad resonance behavior and for large fabrication tolerances using a Rigorous-Coupled-Wave Analysis (RCWA) [24]. In case of a very low fill factor of the encapsulated grating, the effective index approaches $n_{\text{eff}} \rightarrow 1$. According to Ineq. (1), the grating period d has to be greater than 443 nm and smaller than 1550 nm since we are interested in a high reflectivity of laser light with the wavelength of $\lambda = 1550\,\text{nm}$ impinging under normal incidence. We chose a grating period of $d = 800\,\text{nm}$ being well within this regime and TE-polarized light (electric field oscillating parallel to the grating ridges). Figure 2(a) shows the calculated reflectivity of the encapsulated grating reflector versus the thickness of the top waveguide layer s ranging from 300 nm to 390 nm for fixed values of the fill factor ($f = 0.4$) and the groove depth ($g = 2\,\mu\text{m}$). The plot reveals a reflectivity of greater than 95 % in the range of $327\,\text{nm} < s < 347\,\text{nm}$ and a value of close to unity ($> 99.99\,\%$) for a thickness of $s = 337\,\text{nm}$. Since the coupling efficiency to the waveguide modes by reflected higher diffraction orders is pretty weak, the tolerance of the top high-index layer thickness s is rather low.

In order to optimize the fabrication tolerances of the encapsulated grating for the design thickness of $s = 337\,\text{nm}$, fill factor and groove depth were varied ranging from $0 < f < 0.6$ and $0 < g < 2\,\mu\text{m}$, respectively. The plotted reflectivity in Fig. 2(c) reveals a wide range of high reflectivity with values $> 95\,\%$ as indicated by the dashed line. Values even exceeding 99.99 % are within the white area. This plot clearly supports the theoretical considerations of the preceding paragraphs. For a fill factor smaller then about 0.5, a minimal groove depth can be found which is required in order to prevent evanescent transmission of higher grating modes to the substrate. If the fill factor is approaching 0.1 the excitation of waveguide modes is too weak to allow for a high resonant reflection.

The optimum encapsulated grating parameter values arising from our rigorous calculations are, at a glance:

$$\begin{array}{rcl} n_{\text{H}} & = & 3.48 \\ \lambda & = & 1550\,\text{nm} \\ \phi & = & 0^\circ \\ d & = & 800\,\text{nm} \end{array} \quad \Longrightarrow \quad \begin{array}{rcl} f & = & 0.4 \\ g & = & 1300\,\text{nm} \\ s & = & 337\,\text{nm}. \end{array} \tag{2}$$

Figure 2(b) shows the simulated spectral response of the design grating device, revealing a 95 % reflectivity for a rather broad wavelength range of $1550\,\text{nm} \pm 25\,\text{nm}$.

#120315 - $15.00 USD Received 23 Nov 2009; revised 16 Dec 2009; accepted 17 Dec 2009; published 18 Dec 2009
(C) 2009 OSA

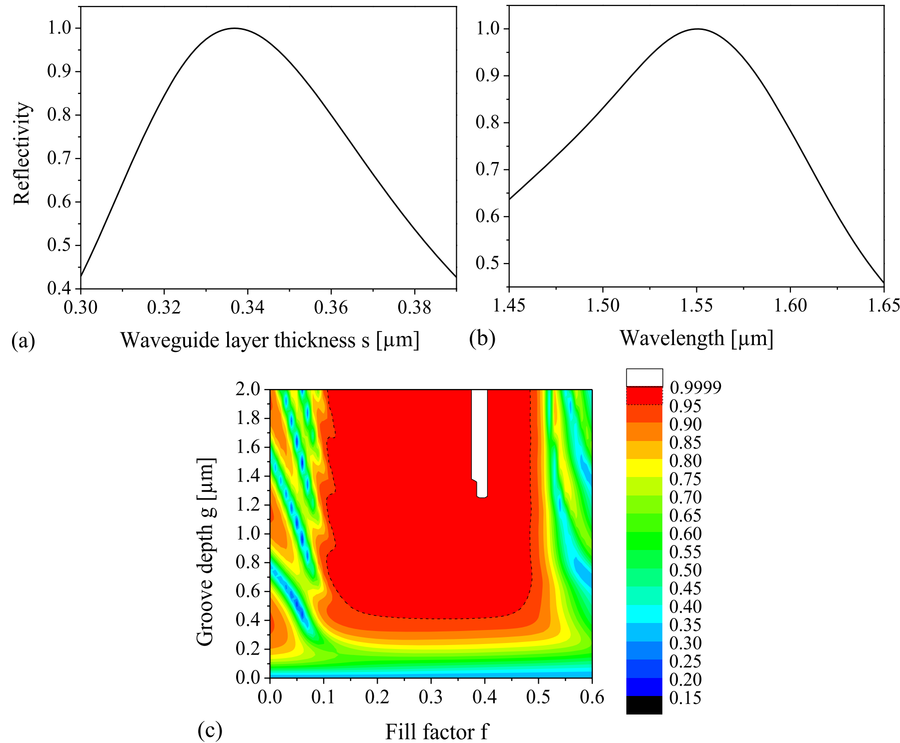

Fig. 2. (a) Calculated reflectivity versus thickness of the top waveguide layer s for fixed values of $d = 800\,\text{nm}$, $f = 0.4$, and $g = 2\ \mu\text{m}$, assuming TE-polarization and normal incidence of light at $\lambda = 1550\,\text{nm}$. (b) Calculated spectral reflectivity for the grating design parameters given in Eqs. (2). (c) Calculated reflectivity over fill factor f and groove depth g for $s = 337\,\text{nm}$.

5. Fabrication process

For the realization of our encapsulated grating, first a conventional surface relief grating was fabricated which was then covered by a homogeneous layer of a certain thickness (superstrate). The superstrate can either be realized by applying wafer direct bonding techniques [25] or by a controlled material deposition without filling the grating grooves [26]. For our device we used the latter approach. A standard silicon wafer with 100 mm in diameter was first coated with a 80 nm chromium layer, serving as the mask during the silicon etching process. After spin-coating an electron beam sensitive (chemically amplified) resist on top, the 800 nm period grating was defined by means of electron beam lithography for an area of (7.5 x 50) mm^2, aiming at a grating fill factor of 0.4. The developed binary resist profile was then transferred into the chromium layer and subsequently into the silicon bulk substrate by utilizing an anisotropic (i.e. binary) ICP (Inductively-Coupled-Plasma) dry etching process. Here, the etching time was adjusted to match the desired groove depth of about 1300 nm. The surface relief grating was then entirely covered by the use of Plasma-Ion-Assisted Deposition (PIAD) under an oblique and fixed angle of about 70° to minimize groove filling. Since the periodic profile is transferred to the coated surface, a final CMP (Chemical-Mechanical-Polishing) step was utilized to planarize the surface and to adjust the homogeneous waveguide layer thickness s.

Figure 3(a) depicts a cross-sectional view scanning electron microscope (SEM) image of

#120315 - $15.00 USD Received 23 Nov 2009; revised 16 Dec 2009; accepted 17 Dec 2009; published 18 Dec 2009
(C) 2009 OSA

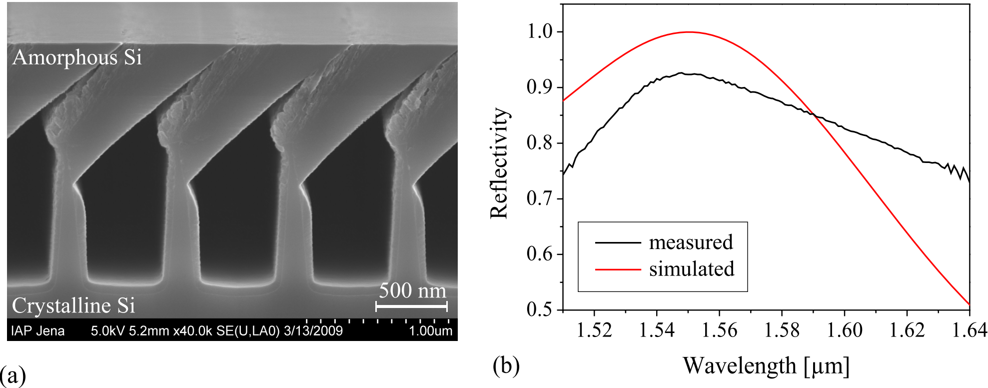

Fig. 3. (a) SEM (scanning electron microscope) cross-sectional view of the fabricated 800 nm period encapsulated grating in silicon that forms a quasi-monolithic surface mirror, efficiently reflecting normally incident light with a wavelength of 1.55 μm. (b) Measured spectral reflectance (black curve) of the fabricated grating for normal incidence $(0 \pm 1)^\circ$ (red curve represents simulation from Fig. 2(b)).

the fabricated and characterized grating profile. Due to the coating process it strongly deviates from the rectangular design structure, however, the high tolerances of our design parameters f and g may still ensure a high reflectivity as demonstrated in the next section. We note that the fabrication technique used here only provides a quasi-monolithic grating as the cover layer has an amorphous structure, see Fig. 3(a). However, in contrast to conventional waveguide gratings our device consists of only one material which suggests a significantly inceased mechanical quality factor [14].

6. Experimental characterization

The spectral reflectivity under normal incidence $(0 \pm 1)^\circ$ was measured using a fiber-coupled tunable diode laser with a spectral range of 1.51 $\mu\text{m} < \lambda < 1.64\,\mu\text{m}$. After the polarized and collimated beam was reflected by the grating, it was deflected onto a photo detector by a beam splitter. As a reference for the measured intensity we used a multilayer dielectric mirror rated at $R = 1$ for the available spectral range. The measured data is shown in Fig. 3(b) (black curve) and reveals a reflectivity of higher than 80 % for a broad spectral range from 1.52 μm to 1.61 μm. The difference between the measured and the simulated data (red curve) is not surprising since the actual fabricated profile also shows substantial differences from the designed profile. Nevertheless, the measured peak reflectivity is located closely to the design wavelength of 1.55 μm with a value of about 93 %, where a measurement error of ± 0.5 % needs to be taken into account. The discrepancy between simulated and measured peak reflectivity of about 7 % is, most likely, mainly attributed to a deviation of the top waveguide layer thickness from its optimum value $s = 337$ nm. From the SEM image in Fig. 3(a), a thickness of 300 nm was estimated. Variations in all the design parameter values might also contribute here. We expect that a major part of the missing 7 % is transmitted through the device. However, this could not be verified since the rear side of the wafer was unpolished. The parameter variations result from inhomogeneities within the various steps of fabrication and need to be further improved by means of technology evaluation.

#120315 - $15.00 USD Received 23 Nov 2009; revised 16 Dec 2009; accepted 17 Dec 2009; published 18 Dec 2009
(C) 2009 OSA

7. Conclusion

Our rigorous modeling has shown that a monolithic flat surface mirror with perfect reflectivity is theoretically possible. Such a reflector comprises an encapsulated subwavelength grating with a flat polished surface and, thus, overcomes the limitations of an earlier approach in Ref. [21] in terms of mechanical stability and device handling. Based on the current understanding of the underlying mechanism of coating thermal noise, such a device should be able to increase the sensitivity in ongoing and future high-precision laser interferometric measurements. We were able to fabricate a first demonstrator of our reflector that consists of a nanostructured crystalline silicon wafer of 100 mm in diameter covered by an amorphous and polished silicon top layer. Our demonstrator showed a high reflectivity of 93 % at the design wavelength of 1550 nm, and represents the first experimental demonstration of a robust, large-area high-reflectivity quasi-monolithic surface. We expect that improvements towards a perfect reflectivity are possible with improved electron beam lithography and other fabrication steps involved. Moreover, we propose to use a wafer direct bonding technique to contact a crystalline top layer (superstrate) onto a crystalline nanostructured substrate, thereby realizing a truly monolithic flat surface reflector.

Acknowledgments

This work was supported by the Deutsche Forschungsgemeinschaft (DFG) within the Collaborative Research Center TR7. The authors would also like to acknowledge Thomas Käsebier and Jens Dreiling for their contributions to the fabrication process.

#120315 - $15.00 USD Received 23 Nov 2009; revised 16 Dec 2009; accepted 17 Dec 2009; published 18 Dec 2009
(C) 2009 OSA